Label-free monitoring of crystalline chitin hydrolysis by chitinase based on Raman spectroscopy

Jun Ando[1,2,3] †, Hiroyuki Kawagoe[1] †, Akihiko Nakamura[2,3,4], Ryota Iino[2,3], Katsumasa Fujita[1,5,6] *

[1]Department of Applied Physics, Osaka University, 2-1 Yamadaoka, Suita, Osaka 565-0871, Japan

[2]Institute for Molecular Science, National Institutes of Natural Sciences, 5-1 Higashiyama, Myodaiji, Okazaki, Aichi 444-8787, Japan

[3]Department of Functional Molecular Science, School of Physical Sciences, SOKENDAI (The Graduate University for Advanced Studies), Hayama, Kanagawa 240-0193, Japan

[4]Department of Applied Life Sciences, Shizuoka University, Shizuoka, Shizuoka 422-8529, Japan

[5]Advanced Photonics and Biosensing Open Innovation Laboratory, AIST-Osaka University, Osaka University, 2-1 Yamadaoka, Suita, Osaka 565-0871, Japan

[6]Institute for Open and Transdisciplinary Research Initiatives, Osaka University, 2-1 Yamadaoka, Suita, Osaka 565-0871, Japan

Corresponding Author

* E-mail: fujita@ap.eng.osaka-u.ac.jp

Author Contributions

† These authors contributed equally to this work.

Abstract

We demonstrate a method for label-free monitoring of hydrolytic activity of crystalline-chitin-degrading enzyme, chitinase, by means of Raman spectroscopy. We found that crystalline chitin exhibited a characteristic Raman peak at 2995 cm^{-1}, which did not appear in the reaction product, *N,N'*-diacetylchitobiose. We used this Raman peak as a marker of crystalline chitin degradation to monitor the hydrolytic activity of chitinase. When the crystalline chitin suspension and chitinase were mixed together, the peak intensity of crystalline chitin at 2995 cm^{-1} was linearly decreased depending on incubation

time. The decrease in peak intensity was inversely correlated with the increase in the amount of released *N,N'*-diacetylchitobiose, which was measured by conventional colorimetric assay with alkaline ferricyanide. Our result, presented here, provides a new method for simple, in-situ, and label-free monitoring of enzymatic activity of chitinase.

Introduction

Chitin is one of the main components of the exoskeletons of insects and crustaceans and the cell walls of fungi[1]. It is a structural polysaccharide composed of *N*-acetyl glucosamine (GlcNAc) linked in β-(1,4) fashion and is generally found as crystalline microfibrils formed by hydrogen bonding among parallel polysaccharide chains. Since a high amount of crystalline chitin exists on the earth, it has been drawing attention as nitrogen-rich biological resources. For biomedical, industrial, and environmental applications, it is necessary to decompose crystalline chitin into small units of chemical compounds[2]. However, due to its stable crystalline structure, harsh thermo-chemical treatment is required for crystalline chitin degradation[3]. On the other hand, in nature, there is an enzyme called chitinase that decomposes crystalline chitin under mild conditions[4-8]. The chitinase, especially well-studied chitinase A from a bacterium *Serratia marcescens* (SmChiA), adsorbs on the surface of crystalline chitin, processively hydrolyzes the β-(1,4) glycosidic bond of the polysaccharide chain, and releases water-soluble reaction product *N,N'*-diacetylchitobiose (Fig. 1). Recent single molecule studies unveiled the operational mechanism of the efficient crystalline chitin degradation by SmChiA, which moves linearly along a single polysaccharide chain like a monorail, and achieves processive hydrolysis governed by biased Brownian motion (burnt-bridge Brownian ratchet)[9-12].

Engineering of the processive chitinase for efficient conversion of crystalline chitin is one of the important research directions. Hydrolytic activity of the chitinase can be further improved by the mutations in amino acid sequences[13-15]. The combination of saturation mutagenesis and robot-based protein purification and activity measurement, which we reported recently, allows us to generate a huge number of site-directed chitinase mutants[16, 17], and provides us more chance to find better mutants with higher activity than the wild-type. To evaluate the hydrolytic activity of various chitinase mutants against crystalline chitin, colorimetric assays have been widely performed with an oxidation

agent, such as ferricyanide[18] and 3,4-dinitrosalicylic acid[19]. In these assays, the amount of released *N,N'*-diacetylchitobiose was monitored by the color change of the reagent, induced by the reduction reaction of *N,N'*-diacetylchitobiose. However, these methods require complicated and time-consuming procedures, such as an addition of colorimetric reagent, heating or boiling of the reaction mixture for color development, and removal of crystalline chitin suspension before colorimetric reaction. These procedures are the bottlenecks to perform high-throughput activity measurement of chitinase mutants. Alternatively, the chromatographic method can be used to monitor the amount of released *N,N'*-diacetylchitobiose[20]. Although chromatographic method does not require an additional reagent, throughput is generally very low, and it also requires the removal of crystalline chitin suspension before measurement. A reagent-free, rapid, and simple assay is highly desired.

Raman spectroscopy provides information on molecular vibration by light. It allows us to identify molecular species without labeling and modification directly. Raman peak intensity of target molecule also provides quantitative information. Furthermore, the spectral shape is sensitive to the structural change of molecules and their surrounding environment. Molecules in liquid can also be analyzed with visible light, allowing us to investigate biomolecules at work in natural conditions. Drawback of Raman spectroscopy has been its weak signal; however, recent advances in detectors, laser sources, and optical filters have largely improved the sensitivity. Furthermore, the spatio-temporal resolution of Raman microscopy has also been improved with the development of a parallel acquisition system that provides hundreds of multiple Raman spectra in a single measurement[21, 22]. These advances allow us to explore a wider range of biological molecules and their activity with Raman spectroscopy in recent years.

In this paper, we demonstrated label-free monitoring of crystalline chitin hydrolysis by chitinase using Raman spectroscopy. We measured Raman spectra of crystalline chitin and *N,N'*-diacetylchitobiose, and identifies a characteristic Raman peak of crystalline chitin that can be distinguished from *N,N'*-diacetylchitobiose. We used this peak as a marker of crystalline chitin degradation to monitor the hydrolytic activity of chitinase. For Raman measurement, we used the slit-scanning Raman microscope we previously developed[22, 23], which can achieve sensitivity high enough to monitor the Raman signal of crystalline chitin at a concentration generally used for conventional biochemical assays. After mixing crystalline chitin and chitinase, we observed the decrease of the Raman peak

intensity of crystalline chitin with the increase of incubation time, which demonstrates that the hydrolytic activity of chitinase is directly monitored by Raman spectroscopy without using any reagents and additional procedures for sample treatment.

Experimental

Preparation of crystalline chitin and chitinases

Crystalline *β*-chitin was purified from tubes of *Lamellibrachia satsuma*. The tubes were cut into pieces about 30 mm, and kept in milliQ water to prevent them from drying out. Eighty grams of the tubes were dipped in 1 L of 1 M sodium hydroxide for a night at room temperature. The tubes were washed by milliQ water, and incubated in 0.3% (w/v) sodium chlorite with 0.1 M sodium acetate (pH 4.9) at 70ºC for 3 h. The tubes were washed again by milliQ water, and incubated in 0.1 M hydrochloric acid at 80ºC for 20 min. After washing by milliQ water, one tenth of the tubes were suspended in milliQ water and homogenized at 10000 rpm by Physcotron (Microtech) until the suspension became homogeneous. Homogenization was repeated more than 9 times, and the suspension was centrifuged at 8000 × *g* for 20 min at 4ºC. The precipitated chitin was kept in 4ºC until next process. Thirty grams of wet chitin were mixed with 120 mL of 6 N hydrochloric acid and 30 mL of milliQ water. Amorphous region of chitin was hydrolyzed at 80ºC for 7 h with agitation at 300 rpm. Two hundred milliliters of milliQ water were added after hydrolysis and incubated for a night. The suspension was centrifuged at 10000-15000 × *g* to precipitate the chitin, and washed by milliQ water until pH of the suspension became neutral. The aggregates were removed by centrifugation at 6000 × *g* for 5 min, and the crystalline chitin suspension was kept at 4ºC. Concentration of the suspension was calculated from the remained weight of 10 mL suspension after dry at 70ºC for a night. Crystallinity was measured by X-ray diffraction using RINT (Rigaku).

Chitinase A and B from a bacterium *Serratia marcescens* (SmChiA and SmChiB) were expressed by *E.* coli Tuner (DE3) strain (Novagen) using a pET27b. His-6 tag was added to C-terminal or N-terminal of SmChiA and SmChiB respectively. Single colony of *E.* coli, containing a plasmid with target gene, was inoculated in 10 mL Luria broth (LB) medium containing 50 μg/mL kanamycin, and incubated at 30ºC for a night. The culture medium was added into 1 liter of LB medium containing 50 μg/mL kanamycin, and incubated at 30ºC until OD_{600} became 2. The medium was cooled on ice for 30 min, and 400 μL of 1 M Isopropyl *β*-D-thiogalactopyranoside (IPTG) was added to the

medium. The medium was further incubated at 20ºC for a night. Cells were harvested by centrifugation at 3000 × *g* for 10 min at 4ºC, and kept in -80ºC after freezing by liquid nitrogen. About 10 g of cell was suspended in 50 mM sodium phosphate buffer (pH 7.0) containing 100 mM sodium chloride, and disrupted by sonication. The suspension was centrifuged at 6000 × *g* for 10 min and then 30000 × *g* for 10 min, and the supernatant was collected. The crude enzyme was loaded to the open column of Ni-NTA resin (5 mL of column volume, Qiagen) and washed by 25 mL of the same buffer without and with 20 mM imidazole. The enzyme was eluted by the same buffer containing 100 mM imidazole, and concentrated by Vivaspin 20 (MVCO 30000, sartorius). The enzyme was loaded into superdex 200 gel filtration column (GE healthcare), and eluted with 20 mM sodium phosphate buffer (pH 7.0) containing 100 mM sodium chloride. The enzyme was concentrated by Vivaspin 20 (MVCO 30000, sartorius).

N,N'-diacetylchitobiose and *N*-acetyl glucosamine were purchased from Megazyme.

Raman measurement

A home-built slit-scanning Raman microscope was employed to measure Raman spectra of the samples[22]. As a light source for Raman measurement, 532 nm laser was utilized (Verdi V-18, Coherent). A cylindrical lens was used to form a line-shaped laser beam, which was focused onto the sample through a water-immersion objective lens (PlanApo IR, 60x, NA 1.27, Nikon). Raman scattering light, generated along the line-shaped laser beam, was collected by the same objective lens and projected onto the slit of imaging spectrometer (MK-300, Bunko Keiki) equipped with a cooled CCD camera (PIXIS 400BeX, Princeton Instruments) after passing through a long pass edge filter (Semrock). The system provided four hundred Raman spectra in parallel. All the spectra in a single measurement were averaged to improve the signal-to-noise ratio. The spectrum was further treated with a moving average filter (window size of 3 pixels, which were equivalent to approximately 9 cm^{-1}) to reduce the noise.

Thirty microliters of sample solution (crystalline chitin, or crystalline chitin with chitinase in 50 mM ammonium acetate buffer, pH 6.0) was dropped on a glass substrate (Glass bottom dish, glass thickness of 0.17 mm, Matsunami) to form a hemispherical droplet. For reference, the same amount of the buffer solution was also dropped on another glass substrate. Raman spectra were acquired from both of these droplets, and then we subtracted the Raman spectrum of buffer solution from that of the sample solution.

The baseline of the crystalline chitin peak at 2995 cm^{-1} was tilted, mainly due to the overlap with neighboring Raman peak at 2945 cm^{-1} and photoluminescence signal from crystalline chitin. For the evaluation of the peak intensity at 2995 cm^{-1}, we defined a straight line from 2978 to 3026 cm^{-1} as a baseline of the peak. The area of the Raman peak beyond the baseline was used as a measure of Raman signal amount of crystalline chitin. For ease to see the peak in Fig. 3b, Fig. 4a and, Fig. 6a, the baseline of the Raman peak was corrected by the straight line from 2978 to 3026 cm^{-1}.

Colorimetric assay for evaluation of hydrolytic activity

Ten microliters of 1 M ammonium acetate buffer (pH 6.0), 100 μL of 4 mg/mL crystalline chitin, 70 μL of milliQ water, and 20 μL of 10 times concentrated enzyme (SmChiA or mixture of SmChiA and SmChiB) were mixed and incubated at 37ºC for an appropriate time. After the reaction, the same volume of Schales' reagent (1.5 mM potassium ferricyanide, 500 mM sodium carbonate) was added to the tube and centrifuged at 15000 × *g* for 5 min at 4ºC. Two hundred fifty microliters of supernatant were transferred to the 8-strip tubes and heated to 98ºC for 15 min by thermal cycler (T100, Bio-rad). The absorbances of reaction mixtures at 420 nm were measured by a plate reader (SpectraMax iD3, Molecular Device), and the concentration of soluble products were calculated according to the standard curve prepared by the same method using 0 to 300 μM of GlcNAc. When the product concentration was over the range of the standard curve, the reaction mixture was diluted.

The soluble product in the reaction mixture after the Raman measurement was determined by the same methods.

Results and Discussion

At first, we measured Raman spectra of 3 mg/mL crystalline chitin suspension and 10 mM *N,N'*-diacetylchitobiose (Fig. 2). The laser intensity was 9.2 mW/μm^2, and the exposure time was 300 s. Since the chemical structures of crystalline chitin and *N,N'*-diacetylchitobiose were almost the same except for the number of repeating units, both of them showed similar spectral shape at both fingerprint and high wavenumber regions, which include vibrational modes of CO/CC stretching (800-1200 cm^{-1}), CH deformation (1200-1500 cm^{-1}), Amide I (~1650 cm^{-1}) and CH stretching (2800-3000 cm^{-1})[24-27].

Among them, we found a characteristic Raman peak at 2995 cm^{-1} in the crystalline chitin, which was not observed in the *N,N'*-diacetylchitobiose. This peak can be assigned to a CH stretching mode of the acetyl group, whose vibration is slightly affected by surrounding hydrogen bonds. The acetyl group of the chitin is highly packed in the crystal. Structural constraints due to hydrogen bonds[28-30] can distort the vibrational mode of acetyl group[24]. We used this peak as a marker to monitor the hydrolysis process of crystalline chitin in chitin-chitinase mixtures by Raman spectroscopy in the latter section. We also measured the Raman spectrum of SmChiA to examine if the Raman signal of chitinase interferes with the detection of crystalline chitin. As shown in Fig. 2, the Raman spectrum of SmChiA did not show a peak at around 2995 cm^{-1} as well as *N,N'*-diacetylchitobiose. Furthermore, the concentration of chitinase in the reaction mixture is constant and quite low at the nanomolar range for biochemical assay[18]. We, therefore, concluded that the background Raman signal from SmChiA is negligible in the Raman-based assay discussed in the latter section.

Next, we evaluated the relationship between crystalline chitin concentration and Raman peak intensity at 2995 cm^{-1}. We used an area of the peak at 2995 cm^{-1} as a measure of Raman signal amount of crystalline chitin (Fig. 3a). To calculate the peak area, we drew a straight line from 2978 to 3026 cm^{-1}, and defined it as the baseline for the peak at 2995 cm^{-1}. The area of the Raman peak above the baseline, shown as the red-shaded region in Fig. 3a, was used as a measure of Raman signal amount of crystalline chitin. Fig. 3b shows representative Raman spectra of crystalline chitin suspensions at various concentrations (0.0 to 8.0 mg/mL), where the baseline was corrected by the straight line from 2978 to 3026 cm^{-1}. Raman peak of crystalline chitin at 2995 cm^{-1} appeared down to a crystalline chitin concentration of 0.25 mg/mL. At each crystalline chitin concentration, Raman spectra were obtained three times. Fig. 3c shows the relationship between crystalline chitin concentration and the area of Raman peak at 2995 cm^{-1}. The red line in Fig. 3c shows a linear fit applied to the dataset of crystalline chitin concentrations from 0.25 to 8.0 mg/mL. Around this concentration range, there was a linear relationship between crystalline chitin concentration and Raman peak at 2995 cm^{-1}, suggesting that the quantitative analysis of crystalline chitin concentration can be performed by Raman spectroscopy. The limit of detection (LOD) of our Raman measurement system for crystalline chitin was 0.18 mg/mL, which was determined by the cross point between the linear fit and the background signal plus three times the standard deviation (SD) of the

background[31]. The background signal was calculated by the measurement without crystalline chitin in solution. For conventional biochemical assay of chitinase with colorimetric analysis, typical crystalline chitin concentration was around 0.5 mg/mL[18]. The sensitivity of our Raman system is therefore sufficient to perform activity assay of chitinases. Within this manuscript, the baseline of the Raman peak was corrected as described above, and the crystalline chitin concentration was calculated by the area of Raman peak at 2995 cm^{-1} with the calibration curve in Fig. 3c.

For comparison, we also evaluated the relationship between crystalline chitin concentration and Raman peak height at 2995 cm^{-1} without baseline correction (Fig. S1). To calculate the peak height, we subtracted the Raman intensity of 3026 cm^{-1} from that of 2995 cm^{-1}. There was a linear relationship between crystalline chitin concentration and the Raman peak height from 0.5 to 8.0 mg/mL, where the red line in Fig. S1 shows a linear fit applied to the dataset at 0.5 mg/mL and higher crystalline concentrations. The LOD of our system with Raman peak height was 0.44 mg/mL, which was determined with the same method as mentioned in previous section[31]. The LOD of our system with baseline-corrected Raman peak area was slightly better than that with Raman peak height. This is presumably because the simple peak height assessment is susceptible to the spectral baseline slope, which were mainly caused by the photoluminescence signal from crystalline chitin and the adjacent Raman peak at 2945 cm^{-1}. To analyze subtle changes in crystalline chitin concentration induced by chitinase, it is better to calculate the peak area using baseline correction than to calculate the peak height.

We then performed Raman measurement of the mixture of crystalline chitin and SmChiA with different incubation times, to verify the capability of our method for monitoring crystalline chitin hydrolysis by chitinase (Fig. 4). In the presence of SmChiA, crystalline chitin is hydrolyzed from its reducing end, and *N,N'*-diacetylchitobiose is released into solution as a reaction product. Prior to Raman measurement, SmChiA and crystalline chitin suspension were mixed together at a final concentration of 400 nM for SmChiA and 2.0 mg/mL for crystalline chitin and incubated at 37ºC for up to 10 hours. After incubation, the mixture was analyzed with Raman spectroscopy. The laser intensity and exposure time were 9.2 $mW/\mu m^2$ and 300 s, respectively. Figure 4a shows Raman spectra of the chitin-chitinase mixtures at different incubation times. The spectral baseline was corrected by the straight line from 2978 to 3026 cm^{-1}, as has been explained above. The Raman peak intensity of crystalline chitin at 2995 cm^{-1} decreased as the incubation

time increased. Figure 4b shows the relationship between the incubation time and the crystalline chitin concentration, calculated by the area of Raman peak at 2995 cm^{-1}. Crystalline chitin concentration, quantified by Raman spectroscopy, decreased with the increased incubation time with chitinase.

To verify if the decrease of Raman intensity at 2995 cm^{-1} in Fig. 4 were correlated with the hydrolytic activity of chitinase, amount of released *N,N'*-diacetylchitobiose was monitored by the conventional colorimetric method with alkaline ferricyanide. Incubation conditions of the chitin-chitinase mixture for colorimetric analysis were same as that for Raman measurement. Red symbols in Fig. 4b represent concentration of the released *N,N'*-diacetylchitobiose in the reaction mixture at different incubation times. The amount of released *N,N'*-diacetylchitobiose increased with the increased reaction time. An anti-correlation relationship was observed between the Raman peak intensity at 2995 cm^{-1} and the concentration of released *N,N'*-diacetylchitobiose, indicating that the decrease of Raman intensity is correlated with the hydrolytic activity of chitinase. To compare the result of Raman measurement and colorimetric analysis, we also back-calculated the released *N,N'*-diacetylchitobiose concentration $C_{chitobiose}\,(t)$ (with the unit of mol/L or M) from the result of Raman measurement using Eq. 1:

$$C_{chitobiose}(t) = \frac{\{C_{initial} - C_{chitin}(t)\}}{424} \qquad (1)$$

where, t is the incubation time, $C_{initial}$ (with the unit of g/L) is the initial concentration of crystalline chitin quantified by Raman measurement, $C_{chitin}\,(t)$ (with the unit of g/L) is the concentration of crystalline chitin quantified by Raman measurement at each incubation time, and 424 (with the unit of g/mol) is the molecular weight of the *N,N'*-diacetylchitobiose. The concentration of released *N,N'*-diacetylchitobiose, back-calculated from the Raman measurement, showed similar values with that from colorimetric analysis (Fig. 5). The initial rate of the *N,N'*-diacetylchitobiose production by SmChiA, quantified by Raman measurement, was 0.82 mM/h (corresponding to 0.57 s^{-1} as the hydrolytic activity of SmChiA), which was calculated by a linear fit to the black symbols in Fig. 5 with an incubation time from 0 to 4 hours. We confirmed that our Raman measurement was consistent with the conventional colorimetric analysis and captured the hydrolytic activity of chitinase on crystalline chitin without any labeling and complicated procedures.

In addition, we performed Raman-based chitin hydrolysis measurement with a mixture of SmChiA and *Serratia marcescens* chitinase B (SmChiB) (Fig. 6). In contrast to SmChiA, SmChiB hydrolyzes crystalline chitin from a non-reducing end. It has been reported that the mixture of SmChiA and SmChiB shows a synergistic effect on crystalline chitin degradation, presumably because of their opposite directionalities of chitin hydrolysis[4]. Investigation of the mechanism underlying the synergistic effect in detail is important for efficient degradation of crystalline chitin. Here we verified whether our method could be used for the analysis of the mixture of these two different chitinases. Prior to the activity measurement, we obtained the Raman spectrum of SmChiB. The Raman spectrum of SmChiB did not show a peak at around 2995 cm^{-1}, confirming that the Raman signal of SmChiB also does not interfere with the detection of crystalline chitin (Fig. S2). Crystalline chitin suspension was then mixed with both SmChiA and SmChiB at a final concentration of 2.0 mg/mL for crystalline chitin and 400 nM for both of the enzymes and incubated at 37ºC for up to 90 min. Raman spectra and estimated concentration of crystalline chitin in the mixtures are shown in Fig. 6. Same as the previous experiment, the Raman signal of crystalline chitin decreased with the increased incubation time (Fig. 6a), and the amount of released *N,N'*-diacetylchitobiose concentration, back-calculated from the Raman measurement, was consistent with that from colorimetric analysis (Fig. 6b, Fig. 7). In the SmChiA-SmChiB mixture, crystalline chitin was hydrolyzed more rapidly than in the SmChiA, and almost all crystalline chitin was degraded within 90 min. The initial rate of the *N,N'*-diacetylchitobiose production by SmChiA-SmChiB mixture, quantified by Raman measurement, was 5.16 mM/h, which was calculated by a linear fit to the black symbols in Fig. 7 with an incubation time from 0 to 30 min. Initial rate of the *N,N'*-diacetylchitobiose production of SmChiA-SmChiB mixture (400 nM for both of the enzymes) was 6.3 times higher than that of SmChiA (400 nM), although total enzyme concentration was only 2 times higher. Furthermore, considering the total enzyme concentration of SmChiA-SmChiB mixture (800 nM), the hydrolytic activity was estimated to be 1.8 s^{-1}. This value was 3 times higher than that for only SmChiA (0.57 s^{-1}). These results clearly indicate the synergistic effect. We confirmed that the Raman-based activity measurement developed in this research is feasible for analyzing the mixture of the different chitinases quantitatively.

In this study, we used Raman microscope to analyze hydrolytic activity of chitinase against crystalline chitin. Under the microscopic observation with single objective lens,

only one droplet with the volume of 30 μL (30 mm^3), containing chitin-chitinase mixture, can be measured at a time. Therefore, total measurement time will be linearly increased with the number of chitinase mutants. The exposure time for the Raman analysis of crystalline chitin was 300 s in this study. For high-throughput activity measurement of chitinase mutants, which handles several tenth to hundreds of samples, long measurement time more than several hours will be required in total. To shorten the total measurement time, we have recently been developing a multi-focus Raman measurement system that is compatible with widely used 384-well microplate[32]. It allows us to detect Raman signals of multiple samples from 192 wells at the same time with multiple objective lens. In principle, Raman-based assay of chitinase activity, presented here, can also be performed on this system, reducing the measurement time for multiple chitinase mutants by over 100-fold. Furthermore, Raman-based assay does not require any sample pre-treatment or reagents for activity measurement, which can shorten the time for sample preparation. Combination of Raman-based activity measurement method and parallel acquisition system will have a potential to drastically shorten the total screening time for chitinase activity compared with conventional colorimetric assay.

Colorimetric measurement of the chitinase activity on crystalline chitin has to be performed as endpoint assays because sample heating or boiling is required for the color development. To analyze the time-dependence of the hydrolytic activity of chitinase against crystalline chitin in detail, a large number of endpoint assays will be required. On the other hand, Raman-based activity measurement of chitinase can, in principle, be performed continuously with the same sample solution, which will largely shorten the measurement time. However, continuous measurement with the Raman system is currently limited because of the precipitation of the crystalline chitin suspension. The stirring system of the sample solution will avoid the precipitation of the crystalline chitin during Raman measurement. With an improvement of the Raman measurement system, hydrolytic activity of chitinase against crystalline chitin can be continuously monitored by Raman spectroscopy.

Conclusions

In this paper, we demonstrated label-free monitoring of crystalline chitin hydrolysis by chitinase based on Raman spectroscopy. We found that the characteristic Raman peak of crystalline chitin appears at 2995 cm^{-1}, which can be distinguished from that of reaction

product *N,N'*-diacetylchitobiose. Raman peak intensity of 2995 cm^{-1} showed a linear relationship with a concentration of crystalline chitin, enabling us to perform quantitative evaluation of crystalline chitin hydrolysis by chitinase with Raman spectroscopy. LOD of our system for crystalline chitin detection was 0.2 mg/mL, which can analyze crystalline chitin at a typical concentration used for the colorimetric assay. To validate the proposed method, we performed Raman measurements of the mixture of crystalline chitin and chitinase with different incubation times. As a result, Raman intensity at 2995 cm^{-1} was decreased with increased incubation time. The initial rate of the *N,N'*-diacetylchitobiose production by SmChiA, quantified by Raman measurement, was 0.82 mM/h, which corresponds to hydrolytic activity of SmChiA at 0.57 s^{-1}. Furthermore, the synergistic effect of SmChiA-SmChiB mixture was quantitatively analyzed. These results show that Raman spectroscopy can monitor the hydrolytic activity of chitinase against crystalline chitin without any additional reagents and sample pre-treatments. Our developed method is not limited to an assay for chitin-chitinase mixture and can be applied to various enzymes which have characteristic Raman peaks in either substrates or products. It will pave the way to perform activity measurements of various enzymes in a high-throughput and label-free manner.

Figures and figure legends

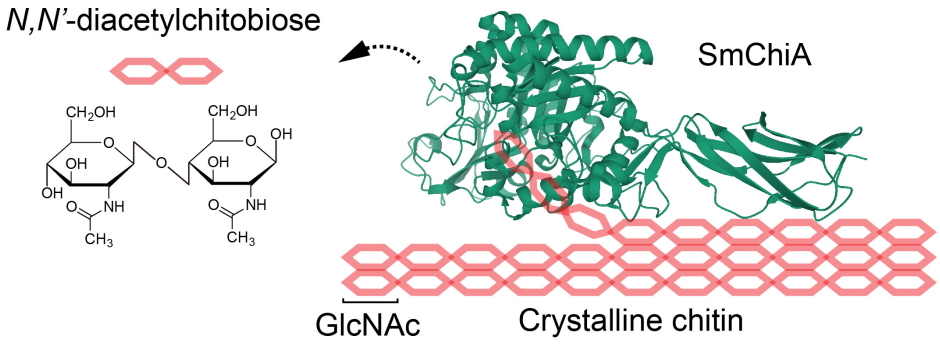

Fig. 1 Schematic of crystalline chitin, *N,N'*-diacetylchitobiose, and chitinase A from a bacterium *Serratia marcescens* (SmChiA). The SmChiA adsorbs on the surface of crystalline chitin and processively hydrolyzes a polysaccharide chain of chitin. *N,N'*-diacetylchitobiose, a dimer of GlcNAc, is released in solution as a reaction product. The SmChiA achieves processive hydrolysis by linearly moving along the polysaccharide chain.

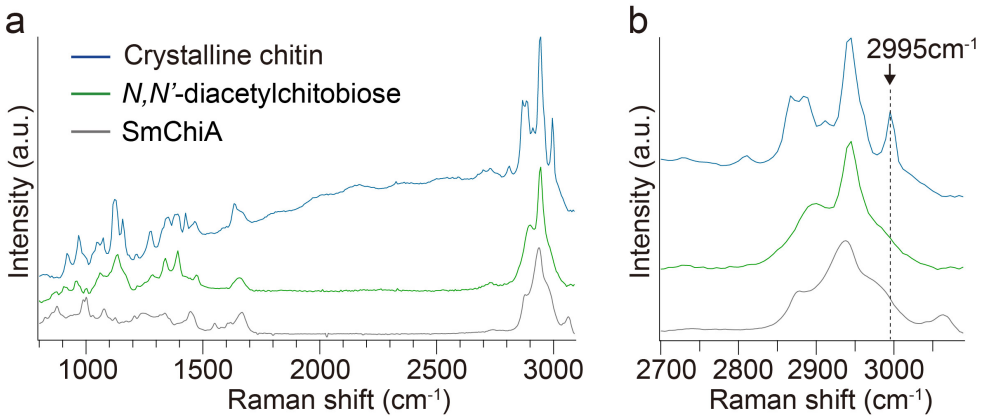

Fig. 2 Raman spectra of crystalline chitin, *N,N'*-diacetylchitobiose and SmChiA at a spectral range between (a) 800 and 3089 cm^{-1}, and (b) 2700 and 3089 cm^{-1}. The black arrow indicates characteristic Raman peak of crystalline chitin at 2995 cm^{-1}. The concentrations of crystalline chitin, *N,N'*-diacetylchitobiose and SmChiA were 3 mg/mL, 10 mM, and 100 μM, respectively.

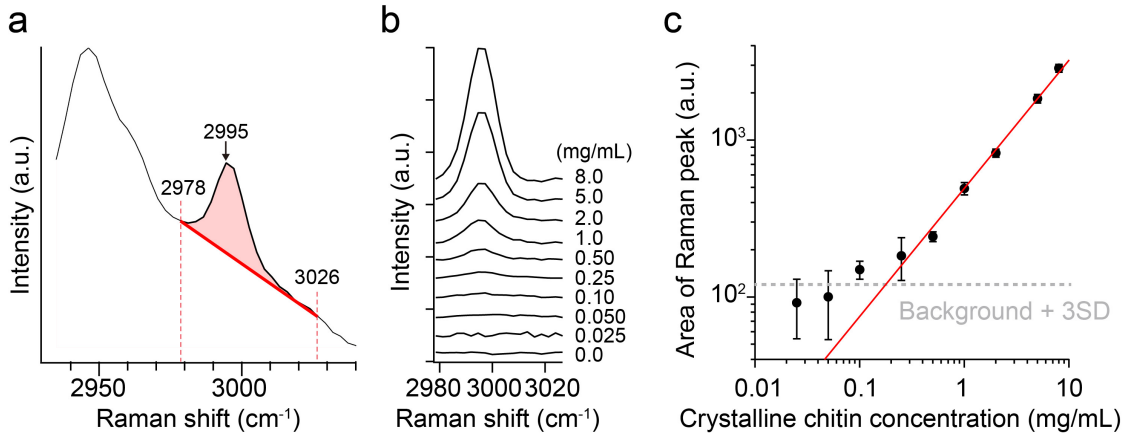

Fig. 3 Relationship between Raman peak intensity of 2995 cm^{-1} and crystalline chitin concentration. (a) Schematic of the measurement of Raman peak area of 2995 cm^{-1}. The red shaded area above the red straight line from 2978 to 3026 cm^{-1} was evaluated as the area of the Raman peak. (b) Representative Raman spectra of crystalline chitin at different concentrations. The baseline was corrected by the straight line from 2978 to 3026 cm^{-1}. (c) Relationship between crystalline chitin concentration and area of Raman peak at 2995 cm^{-1}. The red line represents a linear fit applied to the dataset of crystalline chitin concentrations from 0.25 to 8.0 mg/mL. Error bars represent SD (n=3). The gray dotted line represents a level of background signal plus three times SD of the background.

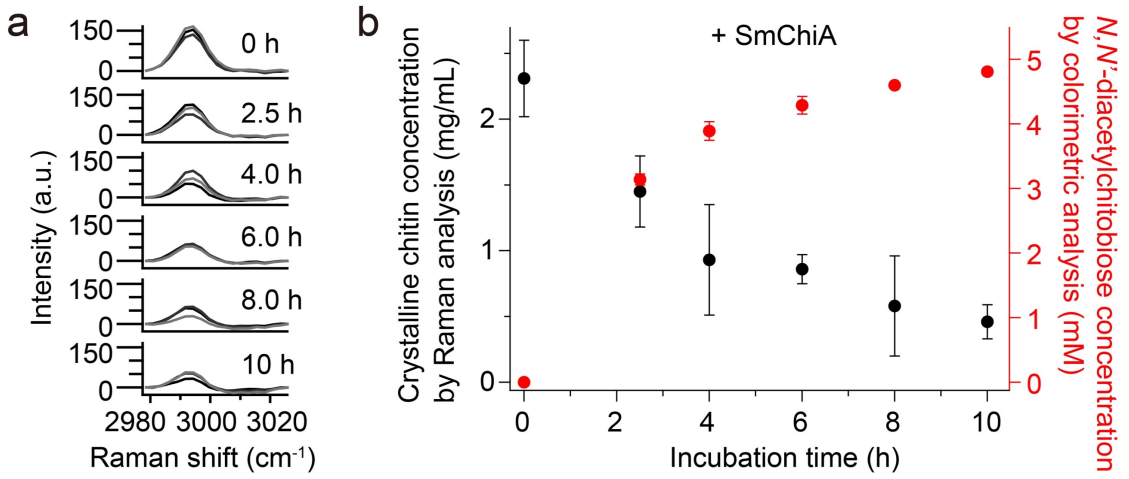

Fig. 4 Raman spectroscopic observation of crystalline chitin hydrolysis by SmChiA. (a) Raman spectra of the mixture of crystalline chitin and SmChiA at different incubation times. (b) Incubation time dependences of crystalline chitin concentration (black symbols) and *N,N'*-diacetylchitobiose concentration (red symbols) for the chitin-SmChiA mixture. The concentrations of crystalline chitin and *N,N'*-diacetylchitobiose were quantified by Raman spectroscopy and colorimetric measurement with alkaline ferricyanide, respectively. Error bars represent SD for both crystalline chitin concentration with Raman analysis and *N,N'*-diacetylchitobiose concentration with colorimetric analysis (n=3).

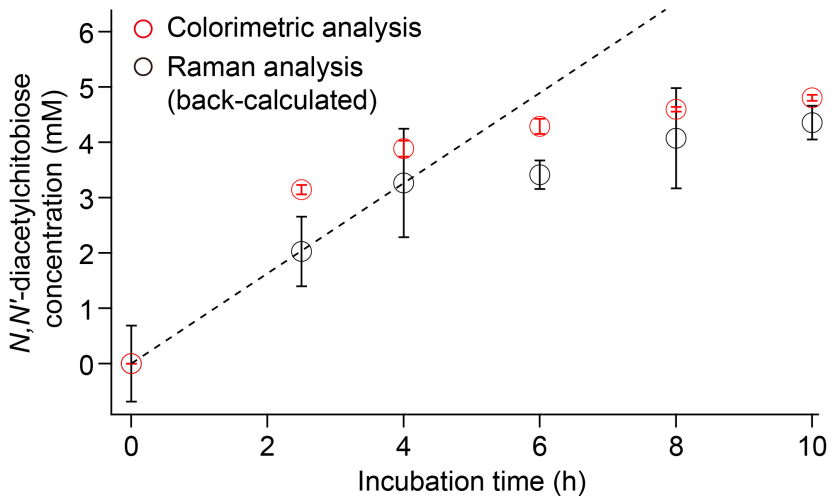

Fig. 5 Concentration of released *N,N'*-diacetylchitobiose in chitin-SmChiA mixture quantified by colorimetric analysis (red symbols) and Raman analysis (black symbols) with back-calculation. For Raman analysis, released *N,N'*-diacetylchitobiose concentration was back-calculated with Eq. 1 in the manuscript. The black dotted line represents a linear fit applied to the dataset of back-calculated *N,N'*-diacetylchitobiose concentrations with an incubation time from 0 to 4 hours. Error bars represent SD for both *N,N'*-diacetylchitobiose concentration with colorimetric analysis and back-calculated *N,N'*-diacetylchitobiose concentration with Raman analysis (n=3).

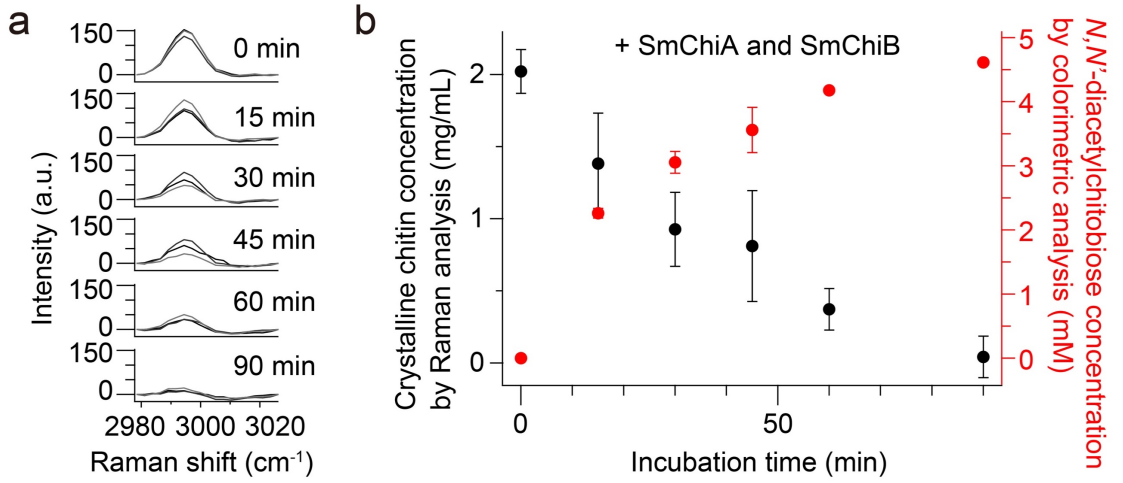

Fig. 6 Raman observation of synergistic crystalline chitin hydrolysis by SmChiA and SmChiB. (a) Raman spectra of the mixture of crystalline chitin, SmChiA, and SmChiB at different incubation times. (b) Incubation time dependences on crystalline chitin concentration (black symbols) and *N,N'*-diacetylchitobiose concentration (red symbols) for the chitin-SmChiA-SmChiB mixture. The concentrations of crystalline chitin and *N,N'*-diacetylchitobiose were quantified by Raman spectroscopy and colorimetric measurement with alkaline ferricyanide, respectively. Error bars represent SD for both crystalline chitin concentration with Raman analysis and *N,N'*-diacetylchitobiose concentration with colorimetric analysis (n=3).

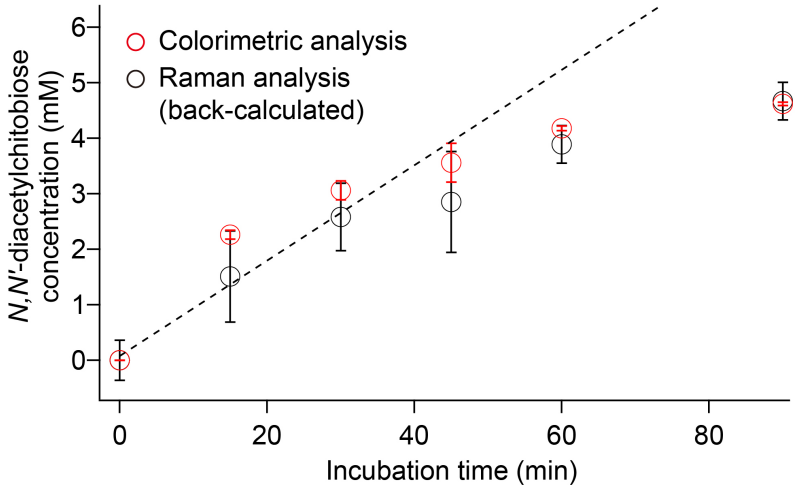

Fig. 7 Concentration of released *N,N'*-diacetylchitobiose in chitin-SmChiA-SmChiB mixture quantified by colorimetric analysis (red symbols) and Raman analysis (black symbols) with back-calculation. The black dotted line represents a linear fit applied to the dataset of back-calculated *N,N'*-diacetylchitobiose concentrations with an incubation time from 0 to 30 min. Error bars represent SD for both *N,N'*-diacetylchitobiose concentration with colorimetric analysis and back-calculated *N,N'*-diacetylchitobiose concentration with Raman analysis (n=3).

Conflicts of interest

There is no conflict of interest to be declared.

Author contributions

J.A., R.I. and K.F. designed the research; J.A. and H.K. performed Raman measurement and data analysis; A.N. prepared the sample and carried out colorimetric analysis; All authors discussed the data; J.A., H.K., and A.N. prepared the draft of the manuscript, and R.I. and K.F. reviewed and revised the manuscript.

Acknowledgements

This work was partially supported by the grant of Joint Research by the National Institutes of Natural Sciences (NINS; NINS program No. 01111704 to K.F. and R.I.), the grant of AMED-CREST under Grant JP18gm071000, the Grants-in-Aid for Scientific Research on Innovative Areas “Molecular Engine” (grant number JP18H05424 to R.I.), and the Grants-in-Aid for Scientific Research (19H03094 to A.N., and JP18H02418, JP18H04755 to R.I.) from the Ministry of Education, Culture, Sports, Science, and Technology of Japan.

References

1. M. Barikani, E. Oliaei, H. Seddiqi and H. Honarkar, *Iranian Polymer Journal*, 2014, **23**, 307-326.
2. M. J. Hülsey, *Green Energy & Environment*, 2018, **3**, 318-327.
3. A. Einbu and K. M. Vårum, *Biomacromolecules*, 2008, **9**, 1870-1875.
4. K. Suzuki, N. Sugawara, M. Suzuki, T. Uchiyama, F. Katouno, N. Nikaidou and T. Watanabe, *Bioscience, biotechnology, and biochemistry*, 2002, **66**, 1075-1083.
5. H. Zakariassen, B. B. Aam, S. J. Horn, K. M. Vårum, M. Sørlie and V. G. H. Eijsink, *Journal of Biological Chemistry*, 2009, **284**, 10610-10617.
6. A. Perrakis, I. Tews, Z. Dauter, A. B. Oppenheim, I. Chet, K. S. Wilson and C. E. Vorgias, *Structure (London, England : 1993)*, 1994, **2**, 1169-1180.
7. Y. Papanikolau, G. Prag, G. Tavlas, C. E. Vorgias, A. B. Oppenheim and K. Petratos, *Biochemistry*, 2001, **40**, 11338-11343.
8. M. Kurašin, S. Kuusk, P. Kuusk, M. Sørlie and P. Väljamäe, *Journal of Biological Chemistry*, 2015, **290**, 29074-29085.
9. K. Igarashi, T. Uchihashi, T. Uchiyama, H. Sugimoto, M. Wada, K. Suzuki, S. Sakuda, T. Ando, T. Watanabe and M. Samejima, *Nature Communications*, 2014, **5**, 3975-3977.
10. A. Nakamura, K.-i. Okazaki, T. Furuta, M. Sakurai and R. Iino, *Nature Communications*, 2018, **9**, 3814-3812.
11. K.-i. Okazaki, A. Nakamura and R. Iino, *The Journal of Physical Chemistry B*, 2020, **124**, 6475-6487.
12. A. Nakamura, K.-i. Okazaki, T. Furuta, M. Sakurai, J. Ando and R. Iino, *Biophysics and physicobiology*, 2020, **17**, 51-58.
13. A. Oyeleye and Y. M. Normi, *Bioscience reports*, 2018, **38**.
14. T. Liu, L. Chen, Y. Zhou, X. Jiang, Y. Duan and Q. Yang, *Journal of Biological Chemistry*, 2017, **292**, 2080-2088.
15. A. Visootsat, A. Nakamura, P. Vignon, H. Watanabe, T. Uchihashi and R. Iino, *Journal of Biological Chemistry*, 2020, **295**, 1915-1925.
16. F. Kawai, A. Nakamura, A. Visootsat and R. Iino, *ACS omega*, 2018, **3**, 7715-7726.
17. A. Visootsat, A. Nakamura, T.-W. Wang and R. Iino, *ACS omega*, 2020, **5**, 26807-26816.

18. A. Nakamura, T. Tasaki, Y. Okuni, C. Song, K. Murata, T. Kozai, M. Hara, H. Sugimoto, K. Suzuki, T. Watanabe, T. Uchihashi, H. Noji and R. Iino, *Physical Chemistry Chemical Physics*, 2018, **20**, 3010-3018.
19. N. Annamalai, M. Veeramuthu Rajeswari, S. Vijayalakshmi and T. Balasubramanian, *Annals of microbiology*, 2011, **61**, 801-807.
20. T. N. Tran, C. T. Doan, M. T. Nguyen, V. B. Nguyen, T. P. K. Vo, A. D. Nguyen and S.-L. Wang, *Polymers*, 2019, **11**.
21. J. Ando, A. F. Palonpon, M. Sodeoka and K. Fujita, *Current opinion in chemical biology*, 2016, **33**, 16-24.
22. A. F. Palonpon, J. Ando, H. Yamakoshi, K. Dodo, M. Sodeoka, S. Kawata and K. Fujita, *Nature protocols*, 2013, **8**, 677-692.
23. K. Hamada, K. Fujita, N. I. Smith, M. Kobayashi, Y. Inouye and S. Kawata, *Journal of biomedical optics*, 2008, **13**, 044027.
24. Y. Ogawa, C. M. Lee, Y. Nishiyama and S. H. Kim, *Macromolecules*, 2016, **49**, 7025-7031.
25. B. Focher, A. Naggi, G. Torri, A. Cosani and M. Terbojevich, *Carbohydrate Polymers*, 1992, **17**, 97-102.
26. C. Y. She, N. D. Dinh and A. T. Tu, *Biochimica et Biophysica Acta*, 1974, **372**, 345-357.
27. E. Wiercigroch, E. Szafraniec, K. Czamara, M. Z. Pacia, K. Majzner, K. Kochan, A. Kaczor, M. Baranska and K. Malek, *Spectrochimica acta. Part A, Molecular and biomolecular spectroscopy*, 2017, **185**, 317-335.
28. J. Kumirska, M. Czerwicka, Z. Kaczyński, A. Bychowska, K. Brzozowski, J. Thöming and P. Stepnowski, *Marine drugs*, 2010, **8**, 1567-1636.
29. J. Cui, Z. Yu and D. Lau, *International journal of molecular sciences*, 2016, **17**.
30. D. Sawada, Y. Nishiyama, P. Langan, V. T. Forsyth, S. Kimura and M. Wada, *PloS one*, 2012, **7**, e39376.
31. S. H. Kim, S. Iwai, S. Araki, S. Sakakihara, R. Iino and H. Noji, *Lab on a chip*, 2012, **12**, 4986-4991.
32. H.-X. Liao, H. Kawagoe, K. Bando, J. Ando, M. Asanuma, K. Dodo, M. Sodeoka and K. Fujita, presented in part at the 2020 Opto-Electronics and Communications Conference (OECC). (DOI: 10.1109/OECC48412.2020.9273699)